Case Studies in Thermal Engineering 41 (2023) 102630

Contents lists available at ScienceDirect

Case Studies in Thermal Engineering

journal homepage: www.elsevier.com/locate/csite

Thermal insulation capability of nanostructured insulations and their combination as hybrid insulation systems

Ákos Lakatos

University of Debrecen, Faculty of Engineering, Department of Building Services and Building Engineering, 4028, Debrecen, Ótemető Str 2-4, Hungary

HIGHLIGHTS

- New theoretical models for the thermal conduction in nano-structured materials (aerogel-graphite enhanced EPS).
- Comprehensive analysis of the thermal properties of nano-technological insulations (specific heat capacity and thermal conductivity).
- Analysis of the hygric properties.
- Analysis of the use of the materials as hybrid insulations.
- Infrared analysis of the energy transport.

GRAPHICAL ABSTRACT

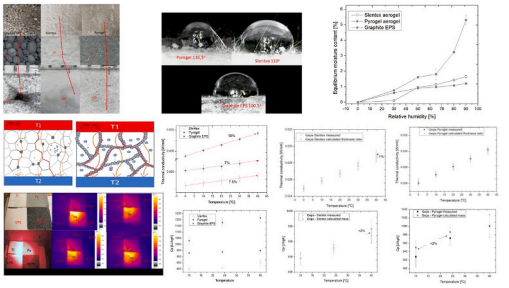

ARTICLE INFO

Keywords:
Thermal conductivity
Graphite polystyrene
Aerogels
Microscopy
Specific heat capacity

ABSTRACT

The applications of insulation materials in buildings and vehicles are more important than ever. Therefore, the application of thermal insulation materials having high-performance heat-blocking properties such as nano-structured insulations like aerogels and graphite polystyrene is essential. In this paper a comprehensive thermal characterization will be presented, executed on two types of fibrous aerogels (slentex, pyrogel) as well as on graphite-expanded polystyrene, to compare their thermal insulation capability. Moreover, their possible sandwich-structured application as hybrid insulation systems was tested, too. The surface analysis of the samples is going to be presented through microscopic and wetting experiments. Thermal conductivity as well as specific heat capacity measurement results of both individual and sandwich structures will be shown. Slentex aerogel has the lowest thermal conductivity and performed best of all. The results of the hybrid structures are promising. The moisture uptake of the pyrogel aerogel is the highest. Based on the measured values theoretical models will be applied for validation, moreover, a face-to-face analysis will also be presented. Furthermore, calculations regarding thermal properties will also be highlighted. Results of both infrared absorption tests and differentiated scanning calorimetry would help the decision makers and it proves the high infrared absorption of graphite polystyrene.

E-mail address: alakatos@eng.unideb.hu.

https://doi.org/10.1016/j.csite.2022.102630
Received 12 October 2022; Received in revised form 23 November 2022; Accepted 6 December 2022
Available online 17 December 2022

Nomenclature

Symbol	*Property*	*Unit*
λ	Thermal conductivity	W/mK
σ	Stefan-Boltzmann Constant	W/(m^2K^4)
n_t	Refractive index	
α_R	Rosseland average absorption (extinction) coefficient	
β	Molecule-wall collisions coefficient	
Kn	Knudsen number	
Θ_{mean}	free mean path	nm
δ	pore size	nm
ν	speed of sound	m/s
T	Temperature	^oC
C_p	Specific heat capacity	J/kgK
t	Time	s
C_{eff}	Volumetric heat capacity	J/Km^3
D_T	Diffusivity	m^2/s
A	Area	m^2
d	Thickness	cm
ρ	Density	kg/m^3
F_T	Temperature conversion factor	
f_T	Temperature conversion coefficient	
m	Mass	g
e	Effusivity	[J/$m^2Ks^{1/2}$]

1. Introduction

Reducing energy losses in the energy sector (buildings, vehicles), especially at the power plant level, is one option for optimizing energy use [1–4]. One way to do this is to use thermal insulation. In some cases, it is not possible to use thermal insulations more than 10 cm thick in buildings, as there is not enough space available, and the outer shell structure of the vehicles also requires the use of "thin" (~2–3 cm thick) thermal insulations [5,6]. Thanks to industrial development, the manufacturing methods of heat insulation materials have also improved. It was reported by Cai et al., Jelle and Schiavoni that, in the last two or three decades one of the most generally applied building insulation materials has been the expanded polystyrene (EPS) foam due to its adequate thermal insulating capability and satisfactory price [7–10]. Lately, new materials have emerged in the marketplace, such as polystyrene foam enhanced with graphite, vacuum insulation panels or aerogel slabs [11–17]. In this context, silica aerogel products are often mentioned as promising materials to increase the thermal resistance of the building envelope. However, despite their outstanding insulating performance, these products are relatively high-priced, and there is little information about their basic thermal properties, strength and long-term performance. Aerogels are supposed to be the next generation of insulation materials [18–21]. In recent years, quite a few scholars have studied nanostructured insulations such as graphite EPS and aerogels. But many of them focused on their individual use and their tests. During this research, I examined nanostructured thermal insulation materials such as graphite-expanded polystyrene and modern (advanced or nanotechnology), but less well-known thermal insulation materials such as aerogels. These materials have nanopores and high porosity, while graphite-enhanced polystyrene insulation foams can be more reliable, because graphite or carbon micro/nanoflakes are added to them during production. Besides their tests, the paper also presents the possible use of their combinations which can be supposed of the novelty of the paper. In general, thermal insulation means the prevention of heat spread between different spaces with various temperatures [12,14,22–24]. Danaci in Ref. [25] made a comparison with REVIT on aerogel and rockwool insulation as systems and reached that with aerogel 8% more energy savings can be reached compared to mineral wool. Kranafti et al. in Ref. [26] presented a comprehensive review of dynamic thermal insulations. They found that dynamic thermal insulation systems can be future solutions from a sustainability point of view. Landolfi presented a comparison of different thermal insulations including external thermal insulation systems (ETICS) [27]. In the absence of sufficient thermal insulation, the heat loss of the system can be significant. The insulation of building services systems and their parts is also important. Pipelines are insulated not only to reduce heat loss, but we also use several insulation methods that serve other purposes as well. Such roles include safety, fire protection, sound attenuation and the prevention of condensation. The thermal insulation coating of the pipeline has several elements that affect not only the efficiency of the system but also the safety of its operation and the resources of the equipment [28–30]. The main aim of the paper is to present both novel measurement and calculation results on individual and sandwich insulations as follows. This paper will present a comprehensive thermal characterization executed on two types of fibrous aerogels as well as on graphite-expanded polystyrene (g-EPS) as a case study. Moreover, their possible sandwich-structured application as hybrid insulation systems will also be presented, where the aerogels are combined with graphite polystyrene. The surface analysis of the samples is presented through microscopic images and wetting experiments. Sorption isotherms with the climatic chamber method as well as the

surface wettability of the samples were explored. Besides the results of the measurements of the thermal conductivity and the specific heat capacity, the experimental results of both the individual and the sandwich structures will be shown executed with Netzsch 446 Heat Flow Meter (HFM) in the function of the temperature. The temperature sensitivity of the thermal conductivities of the samples was also analysed. On the measured results theoretical models are applied for validation. Furthermore, calculations regarding thermal properties such as diffusivity, effusivity and volumetric heat capacity will also be highlighted. Moreover, the results of infrared absorption tests would also help the decision-makers in the preparation of plans, too. With Netzsch Differentiated Scanning Calorimeter (DSC) Sirius 3500 the heat flow is also measured in function of temperature. In this paper, interesting results and applicability suggestions are given regarding the thermal properties of nano-structured insulations and the paper will give suggestions for the possible application of nanostructured insulations as hybrid sandwich structures. Finally, as a comparison of the results, we also provide the literature with a table summarizing the most important properties of the materials. In my opinion, the presented results should be very useful and can extend the available information already presented in these materials. The tested parameters can give reliable basics for designers. These results represent the applicability limits of the materials in different environments (humid or cold/warm). These results give information about the energy-saving potential used for buildings.

1.1. Heat transfer through insulation materials

There are several models for describing the effective thermal conductivity of thermal insulation materials with cellular or fibrous structures. It is a basic fact that in a gas-filled thermal insulation sample the heat spread is separated into four terms: (λ_{cg}) relates to the heat conduction of the gas, (λ_r) expresses the radiation, responsible for the conduction through the solid body (λ_{cs}), and (λ_{conv}) defines the gas convection, the latter being more typical of fibrous materials.

$$\lambda_t = \lambda_{cg}+\lambda_{cs}+\lambda_r+\lambda_{conv} \tag{1}$$

where (λ_t) is the effective thermal conductivity characteristic of the entire bulk material. In our cases the four terms refer to the following, respectively: (a) the heat conduction of the gas occurs from the impact of the gas parts and spreads from particle to particle; (b) the thermal conductivity of the solid part appears as collective lattice vibrations (phonon) as well as through chemical bonds among atoms; (c) the radiative portion can be associated to the electromagnetic energy from the surface of the material in the infrared range, (d) the convection originates from the transportation and movement of air and moisture. These quantities all depend on both temperature or temperature difference and pressure. In the case of cellular objects, the convection value tends to be nil with rising density (decreasing pore size) and becomes negligible.

$$\lambda_t = \lambda_{cg}+\lambda_{cs}+\lambda_r \tag{2}$$

For graphite EPS the λ_r is reduced by the addition of the graphite/carbon flakes.

$$\lambda_r = 16n_t^2\sigma T^3/3\alpha_R \tag{3}$$

where: σ: the Stefan-Boltzmann constant (5.67×10^{-8} W/(m^{2}K^4)); n_t: the refractive index; α_R: the Rosseland average absorption (extinction) coefficient. With the addition of graphite or carbon to the composite during manufacturing, both the Rosseland constant and the n_t refractive index are changed. In materials where the porosity is relatively high, both the convective and conductive parts of the gas contributed heat transfer decreases. If the porosity of a substance rises, the thermal conduction across the solid framework is reduced, since the huge quantity of pores decreases the spread of phonons in the skeleton of aerogel. The impact of the gas part is due to the flexible interactions among particles. The heat conduction of the gas depends both on the length of the mean free path of the gas particles in the pores and on the pore size. The proportion of the mean free path and the pore width is named the Knudsen number (*Kn*), which is described by equation (4). The nanometric size of the pores reduces gaseous convective and conductive heat transfer and radiation.

$$\lambda_{cg} = \lambda_0/(1+2\beta Kn) \tag{4}$$

$$Kn = \Theta_{mean}/\delta \tag{5}$$

where λ_0 is the thermal conduction of the gas in the standard state; β: is the coefficient (1.5–2) used to characterize the energy exchange occurring during molecule-wall collisions (efficiency); δ: is the characteristic pore size (nm); Θ_{mean}: is the free path length of the gas (nm), where gas particles are trapped in the cell (pore) and suffer a collision with the pore wall and not with each other. If the mean free path length of the particles is smaller than the pore (cell) size, the value of the Knudsen number is less than one, otherwise, it is greater than one [31–33].

Another model for specifying the thermal conductivity of nano-porous materials can be given by the following formula:

$$\lambda_d=(\rho_d\nu_d/\rho_0\nu_0)\lambda_1 \tag{6}$$

where λ_1 is the thermal conductivity coefficient of a completely "dense" solid body, ρ_d is the density of the porous material (without pores), ρ_0 is the density of the material without pores, and ν_d is the speed of sound propagation in the porous material and ν_0 is the speed of sound propagation in the material without pores [18,34,35]. The high degree of porosity of aerogel leads to lower density and lower sound propagation speed. Fu presented a critical review on the modelling of the thermal conductivity of silica aerogel composites. For the gaseous thermal conductivity in silica-based composite aerogels empirical and theoretical models were presented. Moreover, for solid conductivity numerical, analytical and empirical forms were also shown [18]. He in Ref. [36] highlights effective

thermal conductivity models for nanostructured insulations. That paper presents a simple volume fraction model for understanding the thermal conductivity of composites. Wang with his colleagues pointed on that the aerogel thermal conductivity can be enhanced by graphene, while it also improves its thermal stability [37]. Among the publications found in the literature regarding the heat conduction equation, I would like to mention the one that describes well how the above relationships can be interpreted in space and time (t, s) if we have temperature-dependent material characteristics:

$$\rho c_p(dT/dt) = \nabla(\lambda\nabla(T)) \tag{7}$$

In this equation, the author assumes that there is no dissipation, the pressure is constant and there is no heat source [38]. In some thermochemical and thermomechanical treatment processes, such as nitriding, it is almost impossible to determine the temperature at the interface with sufficient accuracy. This can only be determined by measuring the temperature inside the solid body and solving the problem inversely. In a non-steady state:

$$\rho[T]c_p[T](dT/dt) = \nabla(\lambda[T]\nabla(T)) \tag{8}$$

It should also be mentioned that the thermal diffusion coefficient (D_T, m^2/s) defined by equation (9) can be used well to describe transient processes [39]. The most significant difference between the two factors (λ and D_T) is their application. While the thermal conductivity coefficient (λ) is mostly used in building physics and building energy to characterize cases that are stable over time (in steady-state), diffusivity (D_T) is used for cases that vary over time, for non-steady or transient cases, where temperature rapidly changing.

$$D_T = \lambda/\rho \times c_p = \ = \lambda/c_{eff} \tag{9}$$

In this formula, ρ is the density of the material measured of the quantity in unit space, c_p defines the absorbed heat of a substance with unit mass during heating (J/kgK) is the specific heat, and C_{eff} (J/m^3K) is the product of these two, the so-called effective heat capacity or volumetric heat capacity defining the heat-storing ability of the substance with unite volume. It must be stated that these are all temperature related in reality. However, while the role of the thermal conductivity factor is well known, the part represented by the above equations can be easily misunderstood. In a material with a high thermal diffusion coefficient, heat quickly passes from the side with a higher temperature to the side with a lower temperature. The above model should be applied in 1 dimension to a homogeneous and isotropic medium in a steady state if the case is independent of temperature and there is no heat source.

In Fig. 1a one can see the heat transfer methods through the fibre-reinforced aerogel. Through the skeleton of the aerogel, the heat can propagate as conduction (λ_{cs}), and from the warm side to the cooler one it transports as an electromagnetic wave (λ_r), while the convection (λ_{conv}) and conduction part of the gaseous thermal conductivity (λ_{cg}), is reduced. Besides this, in Fig. 1b the heat transfer processes are highlighted inside the graphite EPS material. In this case, the conductive part of the heat is transported through both the gas part and the solid phase, while the convective part also exists. However, it is noteworthy that the radiative part of the heat is reduced through partial reflection and absorption on the graphite particles (grey circles) and it is highlighted through the transition of the continuous orange waves to dashed lines.

2. Materials and methods

2.1. Investigated materials

2.1.1. Graphite expanded polystyrene

It was presented earlier that expanded polystyrene (EPS) is a commonly used conventional insulation and a type of it is the graphite enhanced one. EPS is produced in different densities and compressive strengths. Depending on the density (10–35 kg/m^3) it's thermal conductivity can vary in the range of 0.033–0.046 W/mK. Since expanded polystyrene is one of the most widespread thermal insulation materials around the world, the examination of its physical and chemical properties is also a leading topic in international

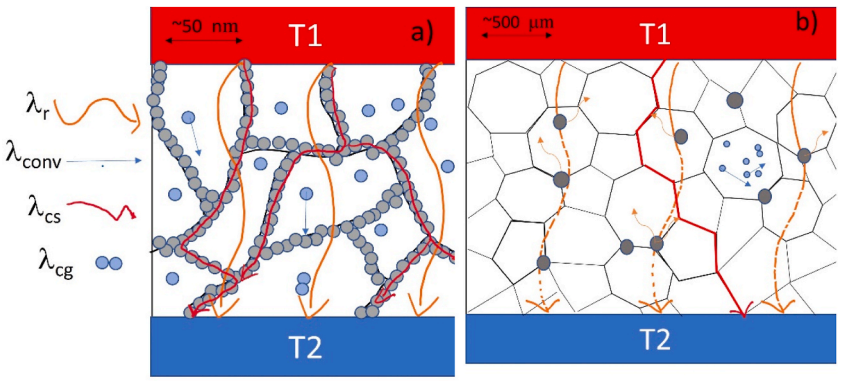

Fig. 1. The heat transfer through the insulation a) fibre-reinforced aerogel and b) graphite-enhanced polystyrene.

research institutes. In addition to conventional thermal insulation materials, the so-called "advanced" (also known as "nano-technological") thermal insulation materials, graphite-doped expanded polystyrene and aerogel-based thermal insulation products are increasingly appearing. For these materials, the "nano-technological" indicator mostly refers to production. The production method of thermal insulation materials doped with graphite is similar to the production of expanded polystyrene, however, when the foaming agent (pentane) is added, micro- and nano-sized graphite powder or carbon black particles are simultaneously added to the melt, thus reducing the material's thermal conductivity. Due to the good ability of graphite to absorb heat radiation, the thermal conductivity of the whole material can be even 20–40% lower than that of "traditional" (white) coloured polystyrene sheets [12,14,23,24]. The graphite-doped thermal insulating material has considerably improved thermal insulation ability, more than the pure white products. It is constructed on polystyrene and small-scale carbon contaminants as an additive in the course of the polymerisation, presented by the research groups of Park and Xiao [40,41]. The carbon additive decreases the radiant heat transport in the cells of the polystyrene and hence the thermal conductivity of the material will be further improved. In the graphite-fixed EPS slab, the infrared (IR) thermal radiation is considerably decreased by the radiation-absorbing and reflective carbon grind particles on the wall of the cell. Zhang et al. presented flame retardancy while Blazejczyk pointed out that, the nano and micro-sized carbon elements play a role as a heat mirror, thereby decreasing the thermal conductivity of the thermal insulation material [42,43].

2.1.2. Aerogels

Silica aerogels are silicon dioxide-based materials, with a dendritic network of silicon-oxid atoms. The preparation of the materials is the following. First, we should fill the fibreglass net with the sol-gel for reinforcement and stability. Secondly, it is super-critical to be extracted with CO_2, and lastly, the fibrous aerogel material is ready to be rolled. The size of the nanopores is smaller than the length of the wave of the IR heat, since their surface reflects and scatters most of the heat [10]. Various products have various thermal conductivity coefficients, but these values are usually less than 0.026 W/mK, which is the thermal conductivity of air at room temperature [11]. They can be produced with different densities of 70–200 kg/m^3 with varying thermal conductivity factors of 0.013–0.025W/mK [19–21]. They have good light transmission and sound insulation. Due to their smaller thermal conductivity, they can also be applied as thermal insulation in smaller widths. The excellent thermal properties of aerogels were also presented [27,28]. During our tests, we examined two different aerogel forms, slentex and pyrogel thermal insulation.

2.1.2.1. Slentex aerogel. This material is a novel high-performance insulating material, non-flammable and flexible. It is practically an improved version of spaceloft aerogel. Slentex is an easy-to-process and non-combustible material, based entirely on mineral raw materials. It is now available as a single-layer, flexible mat for a variety of applications. Slentex thermal insulation is also known as spaceloft A2. Due to these properties, it is mainly used on surfaces where increased fire safety is sought.

2.1.2.2. Pyrogel aerogel. Pyrogel is a high-temperature insulating blanket made from silica aerogel and a non-woven blanket of carbon and fibreglass. Silica aerogels have the lowest thermal conductivity of all known solid materials, but not all of them can be used at 650 °C, which is mandatory for a nuclear power plant. Pyrogel fulfils this criterion, which is why it is a flexible, environmentally friendly and easy-to-use material that is extremely suitable for the thermal insulation of industrial heat transfer systems and ideal for industrial applications. Pyrogel is an essential material for those who want ultimate heat protection. Silica pyrogel is specially designed for pipelines.

The declared and measured properties of the tested materials are highlighted in Table 1 and collected from Refs. [24,44].

2.2. Moisture-related investigations: sorption and hydrophobic experiments

Sorption isotherms of the samples were measured with the combinations of a milligram preciseness balance, with both VentiCell drying equipment and ClimaCell climatic chamber. For the measurements, four samples from each with a 10 cm × 10 cm base area were used, and the final results were the average of the four measurements. The experiments were executed at 23 °C under varied relative humidities (30, 50, 65, 80 and 90%) following the rules presented in EN ISO 12571 standard. Sorption isotherms give information about not only the wetting properties of the samples but their surface microstructure, too [11,45]. With an optical microscope, the surface of the samples was also analysed through hydrophobicity experiments [24].

2.3. Investigations with Netzsch HFM 446 equipment: thermal conductivity and specific heat

Both thermal conductivities and specific heat capacities of the bulk samples with 20 cm × 20 cm base were analysed with a Netzsch Heat Flow Meter 446 S equipment. With this equipment, both the thermal conductivity and the specific heat capacity of thermal insulation materials can be reliably measured. The equipment is calibrated and the accuracy of the measurement results is about 2%.

Table 1
The measured and declared properties of the samples.

Material constants by manufacturer	Graphite EPS	Slentex	Pyrogel
Compressive strength at 10% strain [kPa]	80	30	80
Usage temperature [°C]	<70	400	650
Thermal conductivity at 10 °C [W/mK]	0.031	0.019	0.02
Declared density [kg/m^3]	14–15	185–200	190–200
Fire resistance class	E	A2-s1, d0	A2-s1, d0
Contaminants	C, O, H	C, O, Na, Mg, Al, Si, K, Ca	O, Mg, Al, Si, Ti, Fe, Ca, S
Measured thickness [cm]	2.95	1.02	0.98
Measured density [kg/m^3]	15	188	192

This equipment is supported by a Julabo cooler, to reach the thermal equilibrium of the plates on the samples quickly and reliably. The thermal conductivities of both individual samples (graphite EPS, slentex and pyrogel) and their combinations (graphite EPS-slentex and graphite EPS pyrogel) were measured at 0, 10, 20, 30 and 40 °C mean temperatures with 20 °C temperature differences. The specific heat capacity of both the individual and combined samples was measured at 10, 24 and 40 °C temperatures through a stepwise method of the equipment. To reach both the thermal conductivity and specific heat capacity values three measurement rows were executed [24,28].

2.4. Differentiated scanning calorimetry

Heat flow measurements in the function of temperature were executed with Netzsch Sirius 3500 differentiated scanning calorimeter. The measurements were executed on ground samples having 5–8 mg mass placed in an alumina crucible, in a Nitrogen atmosphere, from 0 °C to 50 °C with 5 K/min heating rate [24].

2.5. Infrared absorption tests

Following the procedure presented in Refs. [24,46,47] infrared (IR) absorption test was executed, too. The samples were placed under a Philips short-wave IR lamp that had 100 W as a source together and their surface temperature during the illumination was registered with a thermo-camera Testo type 868 after 30, 60, 90 and 120 s, IR images were also registered at the mentioned point. On the one hand, the results of this experiment could be a good opportunity to see the possible effects of irradiation on the tested materials. On the other hand, with this experiment, we will show the salient IR absorption property of the graphite polystyrene, presented above (see Fgure 1b).

3. Results and discussion

3.1. Microscopical investigations of samples

In Fig. 2 one can see the optical microscope images of the samples. Firstly, in the top row, the photo image of the samples is visible, graphite EPS, slentex and pyrogel are presented respectively. In the middle row the x5, while in the bottom row the ×20 magnification is highlighted. At the bottom and on the left-hand side one can see that the macro pores are enclosed by the graphite eps beads, moreover, the cellular structure of the micro pores in the beads is also observable. The slentex (white) aerogel has a fibrous structure with a visible inhomogeneous grain size of aerogels. It must be mentioned that the surface structure of the pyrogel (grey aerogel) is also fibrous, but the homogeneity of the visible aerogel grains is higher. As it is visible the structure of the slentex is much blockier.

Fig. 2. Microscope images of the tested samples.

3.2. Results of wetting experiments

In Fig. 3a the measured equilibrium moisture contents in the function of the relative humidity belonging to the samples can be seen. Besides the average values, the standard deviations are also plotted on the graphs. From the curves, we can state that the pyrogel has the highest affinity to take up water among these three materials, while the graphite EPS and the slentex have almost the same affinity. By analysing the shape of the curves, we can state that the pyrogel has a BET III type shape with multilayer bonding of water, while the graphite EPS and slentex have a BET II type shape, with continuous water up taking [48]. The investigation of the effect of moisture is important because strong direct moisture (rain) may hit the sample during construction and the samples can take up water.

Fig. 3b represents the hydrophobicity, namely the surface wettability experiments of the three tested samples. It is visible that all the samples are hydrophobic with more than 90° contact angle. We can state that the contact angles belonging to the aerogels (116.5 and 110°) are significantly greater than the contact angle of the graphite EPS (100°). These observations can be explained by Fig. 2, where it is visible that the aerogels had similar structures (fibres and aerogel grains) with a difference in the order of the grains (the surface of the pyrogel is much more homogenous), which can result in the 10° difference in their contact angles, while the graphite EPS has a purely different cellular surface structure. It is presented in Ref. [49] that the aerogels can be produced in superhydrophobic form, too. Moreover, it was also stated that the hydrophobization of insulation materials is very important [50]. In this paper it also presented that moisture can have a negative effect on the thermal properties of insulation materials such as thermal conductivity. It was also presented in Ref. [11] and Ref. [14]. By adding a hydrophobic protective layer, the durability of the material can be extended. This results in a higher contact angle. If the contact angle is large, the material is more water-repellent.

3.3. Thermal conductivity measurement results and theoretical model

3.3.1. Thermal conductivities of the individual samples

The thermal conductivities of the probes were characterized by Netzsch heat flow meter. Three samples of each were tested. Firstly, the thermal conductivity of the individual samples was measured at 0, 10, 20, 30 and 40 °C mean temperatures, with 20 °C temperature difference. From the results presented in Fig. 4a, we could determine a temperature dependency for all the samples. It is noticeable that aerogels have about 7% increase in thermal conductivity between 0 and 40 °C, while the graphite EPS has about 19%. It shows a strong dependency on the temperature. Thermal conductivities should be tested at different temperatures because the temperature in the structure of the building envelope can fluctuate. Similar results were reached in Ref. [51].

From Fig. 4b according to ISO 10456 standard [52] a temperature conversion coefficient can be reached from the linear fits. This standard provides a procedure to estimate the temperature dependency of the thermal conductivity value of materials between two mean temperatures (T_0 and T_i) by using F_T conversion factor and f_T conversion coefficient.

$$\lambda_T = \lambda_0 \times F_T \tag{10}$$

$$F_T = \exp(f_T \times (T_0\text{-}T_i)) \tag{11}$$

From Equations (10) and (11) by using the natural logarithm one reaches the next equation:

$$\ln(\lambda_T/\lambda_0) = f_T \times \Delta T \tag{12}$$

From the slope of the function plotted by Eq. (12) one can reach the temperature conversion coefficient of the samples. These results are plotted in Fig. 4b. But for comparison, some other results are also given in Table 2. Temperature conversion coefficient can be very useful for designing buildings, during the selection of insulation materials. The smaller the temperature conversion coefficient, the less the thermal conductivity increases as a result of the temperature. During our measurements, we established that for aerogel samples this value can be even half compared to the value of traditional insulation materials (mineral wool, polystyrene).

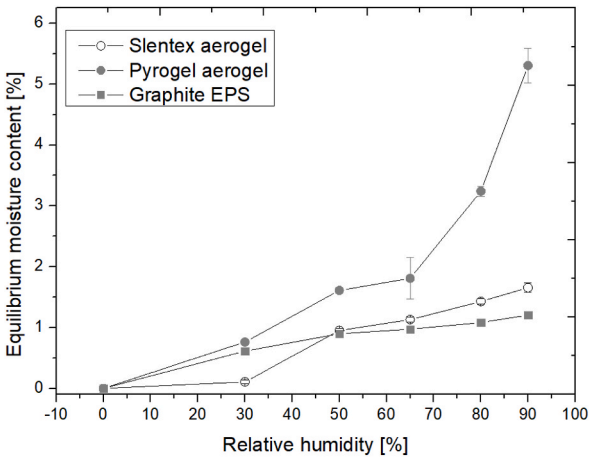

Fig. 3a. The sorption isotherm curves of the samples.

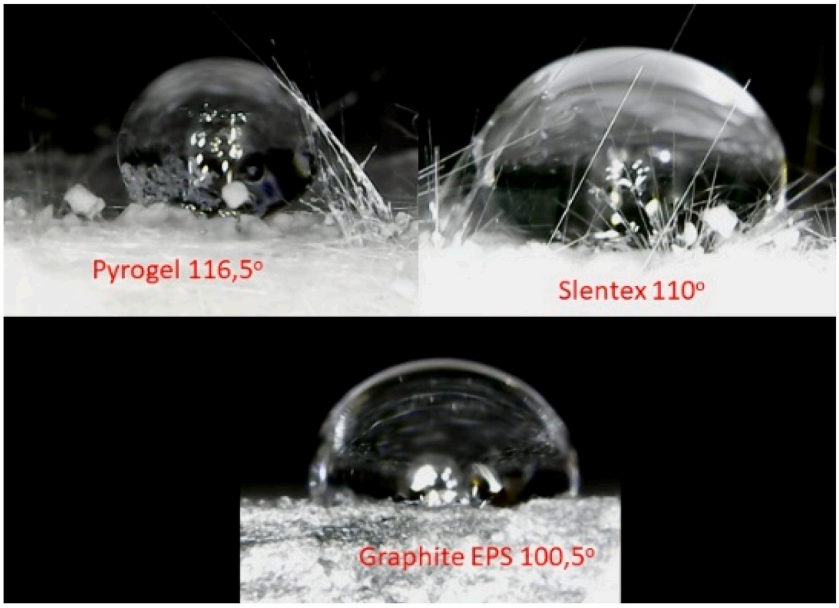

Fig. 3b. The hydrophobic experiments of the samples.

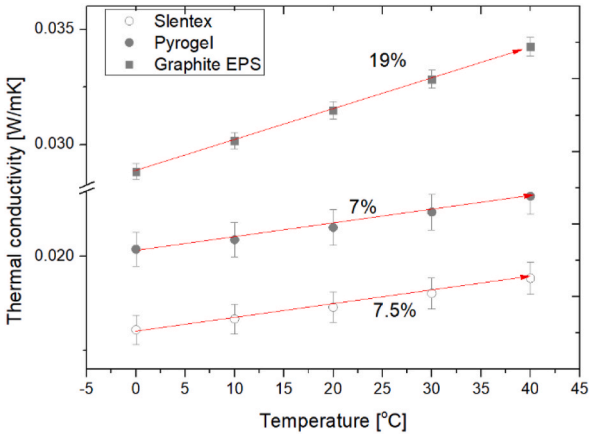

Fig. 4a. Thermal conductivities of the individual samples.

From Table 2 it can be stated that the slentex and pyrogel insulations have lower temperature sensitivity compared to the other materials, while graphite EPS has a close value to the extruded polystyrene. It must be mentioned that these values belonging to the graphite EPS, the slentex and the pyrogel are significant and gap-filling results.

3.3.2. Thermal conductivities of the hybrid-sandwich structured materials

In this section, we present both measurement results and theoretical calculations to reach the thermal conductivity of the sandwich-structured materials. It is well known that the market price of aerogels is high compared to conventional insulations (EPS) as well as in some cases they cannot be produced in large thicknesses (>5 cm). It justifies and gives the feasibility of the use of hybrid-sandwich combinations of conventional insulations with super insulation materials. In both market and literature, the combination of EPS insulations with vacuum insulation panels is well known, therefore in this paper, we try to emphasize the use of the combination of graphite EPS insulation with aerogels as a novel solution. We prepared two sandwich structures from the combinations of aerogels with graphite EPS. This way we reached a graphite EPS-slentex and a graphite EPS-pyrogel sandwich insulations see Fig. 5 and Table 3.

In Fig. 6a and b one can find both the measured and the calculated thermal conductivities. From the measured results one can find that the combination of the graphite EPS with the slentex aerogel results in lower thermal conductivity (0.0248–0.0292) than the sandwich made from the graphite EPS and the pyrogel (0.026–0.0302). For the theoretical approximations of the thermal conductivity of the hybrid structures (λ_h) a theory was applied. Firstly, from the measured thermal conductivities of the individual samples (presented in section 3.3.1) the thermal conductivities of the hybrid structures were calculated [53] by using a thickness fraction model

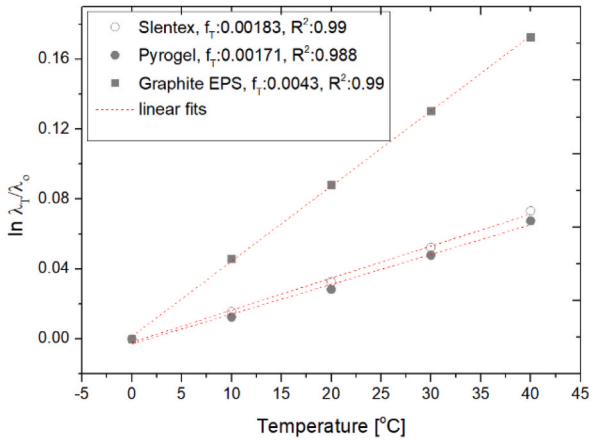

Fig. 4b. The temperature conversion coefficient.

Table 2
Temperature conversion coefficients of materials.

Material	Temperature conversion coefficient
Graphite EPS	0.0043
Slentex (aerogel)	0.00183
Pyrogel (aerogel)	0.00171
Spaceloft (aerogel)	0.0027 [28]
Mineral wool	0.0035 [47]
EPS	0.003–0.0036 [47]
Extruded polystyrene	0.0045 [47]

presented in Eq. (13).

$$\lambda_h = 1/(((d_1/\lambda_1)+(d_2/\lambda_2))/(d_1+d_2)) \quad (13)$$

The results of the calculations are also plotted in Fig. 6a and b. We can state that the thickness fraction model can be a perfect approximation method to reach the thermal conductivity of hybrid sandwich insulations, with the measured values purely analogous to the calculated values.

3.4. Specific heat capacity measurement results and theoretical models

With the Netzsch 446 heat flow meter, besides the characterization of the thermal conductivity, we could measure the specific heat capacity (C_p) of the bulk samples, with the same size samples which we also used for thermal conductivity measurements. In Fig. 7a–c we presented our results with the estimated errors for each measurement row. We measured the C_p values of the individual samples (graphite EPS and the two aerogels). One can see from Fig. 7a that the highest specific heat capacity value belongs to the graphite EPS and a strong increase is deduced in the function of the temperature (10, 24 and 40 °C). The measured value for the pyrogel is about constant, while about a +6% change was manifested for the slentex aerogel.

Fig. 7b and c presents both the measured and calculated C_p values for the hybrid-sandwich structures. For the theoretical approximation of the specific heat capacity of the sandwich materials ($C_{p,h}$) Eq. (14) was used, based on both the measured results presented in Fig. 7a and the measured mass (m) [54].

$$C_{p,h}=(1/(m_1+m_2)) \times ((m_1 \times C_{p1}) +(m_2 \times C_{p2})) \quad (14)$$

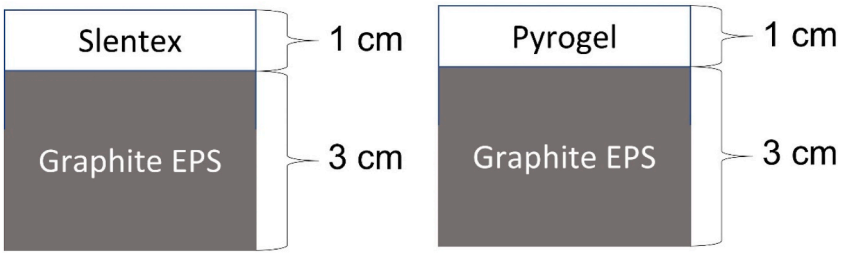

Fig. 5. The sketch of the measured hybrid structures.

Table 3
The parameters of the sandwich structures.

Property	Graphite EPS-Slentex	Graphite EPS-Pyrogel
Density [kg/m^3]	58.75	58.79
Thickness [cm]	3.97	3.93
Mass [g]	93.3	94.4

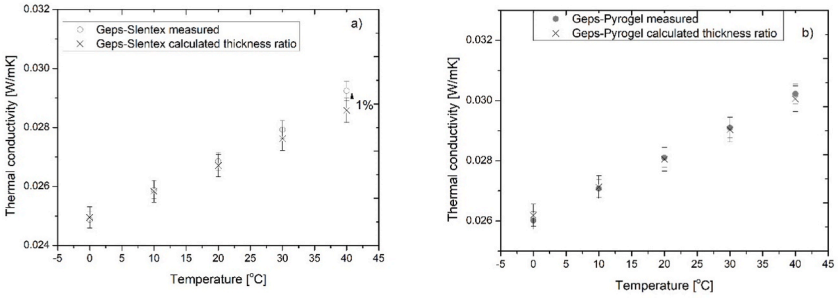

Fig. 6. The thermal conductivity results of a) Geps-slentex sandwich and b) Geps-pyrogel sandwich.

Consequently, we can state that this mass fraction model fits well on the measured values for a pre-estimation of the specific heat capacity of the sandwich samples with about <3% safety. It is also very important to notice that both the measured and the calculated values for the combinations show measurable (~10% increase) between 10 and 40 °C.

3.5. Differentiated scanning calorimetry measurements

With the Netzsch 3500 Sirius differentiated scanning calorimetry experiments were executed on the ground samples. These tests were executed between 0 and 50 °C to see the thermal response of the material against heating. From Fig. 8 we can state that the DSC sign belonging to the graphite EPS shows a continuously increasing trend, which can be in connection with the drying of the sample (dehumidification). While the profile belonging to the aerogels shows a slight hill between 15 and 35 °C and then reaches a constant value. It could be seen that the course of the DSC curve is similar to the course of the cp values presented in Fig. 7a. For graphite EPS both the DSC sign and the Cp values are increasing continuously in the function of the temperature, while the aerogels have a similar flattening hill-like trend.

3.6. Calculations for thermal properties from the measured values

As it is presented above both the calculations and measurements regarding the thermal properties were executed between 0 and 40 °C. Understanding the possible changes in the thermal properties in this temperature range is very important because the temperature profile in building structures can vary between summer and winter in this region in a thermally insulated case. For this, we selected the measured results at 10 and 40 °C for the following reasons. The declared values by the manufacturers are given at 10 °C, while 40 °C is the upper limit value that we applied. Table 4 presents the results of both measurements and calculations at 10 and 40 °C. We calculated the diffusivity, the effusivity and the heat capacity per unit volume. The calculations were executed by using the

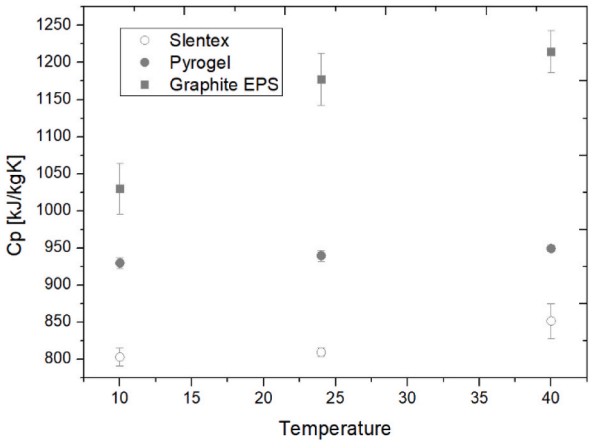

Fig. 7a. The measured specific heat capacities of the individual samples.

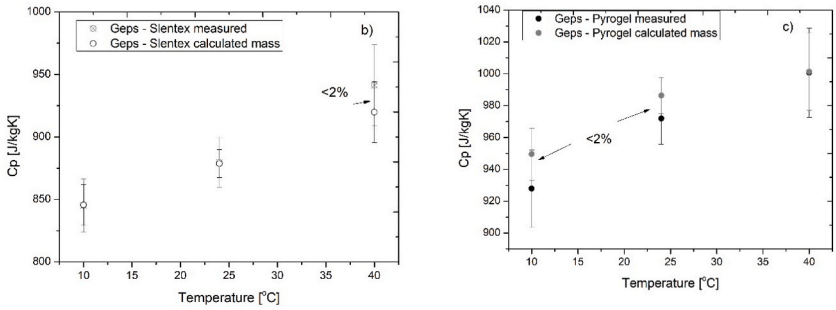

Fig. 7b. The measured and calculated specific heat capacity values of the graphite EPS combined b) with slentex aerogel and c) with pyrogel aerogel.

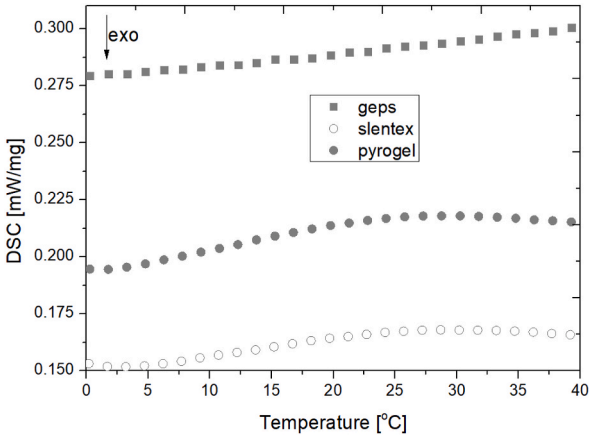

Fig. 8. DSC analysis of the samples.

following equation. The thermal diffusivities (D_T), as well as the effective heat capacities, were found from Eq. (9), while the effusivity (e) was reached from Eq. (15), as

$$e=(\rho \times {}_{cp} \times \lambda)^{0.5} \tag{15}$$

From the calculated data in Table 4 one can conclude that the pyrogel insulation has the highest value of effective heat capacity, followed by the slentex and the graphite EPS both at 10 and 40 °C. The greater the heat capacity of the material, the more heat it can store within itself, which can help in the reduction of the temperature fluctuation in the building structure if the material is applied as insulation on the wall of a building. Furthermore, effusivity is the measure of the material's ability to exchange heat with the environment.

Following the theory presented by Salazar in Ref. [37], Fig. 9 was created. From the λ versus D_T relation one can make a comparison between materials from an insulation capability point of view. It must be mentioned that the best thermal insulation capacity belongs to the smallest values, moreover, the values should reach the origin in the figure. To understand the thermal insulation property we should focus on the left bottom side of Fig. 9, where both the thermal conductivity and the diffusivity are low. It must be mentioned that the diffusivity of the sandwich structured materials approaches the diffusivity values of the individual aerogel samples. The results of these calculations provide a clue for researchers, designers, and decision-makers in the initial state of the construction of buildings and during the material selections. In Ref. [55] it was also presented that the investigation of carbon-based hybrid insulations is vital.

3.7. Infrared absorption tests

Following the research method presented in Refs. [24,44and45], it is worth investigating the infrared absorption of the insulation materials. As Fig. 10a presents, a Philips short-wave IR lamp that had 100 W as a source was used for irradiating the insulating materials. We illuminated a pure white EPS, a graphite EPS as well as the pyrogel and slentex aerogels. During the illumination, we registered the surface temperature with a Testo 868 thermo-camera. With the camera, we took pictures at 30, 60, 90 and 120 s. Fig. 10b presents the IR absorption test. Left-hand side the photo image of the samples before and during the test is presented. In the middle and right-hand side, the IR camera photoshoots are presented with the measured surface temperatures (red temperatures) belonging to M1, M2, M3 and M4 points after 30, 60, 90 and 120 s. From Fig. 10b we can state that the surface temperature of the samples is increasing in the function of the illumination. The starting conditioned temperature was about 28 °C for all samples, which was equal to the temperature of the test room. We observed that at the first 60 s the temperatures raised fast. After 60 s the surface temperatures reached

Table 4
The calculated thermal properties.

10 °C	Diffusivity, D_T [m^2/s]	Effusivity, e [$J/m^2Ks^{1/2}$]	Heat cap. per unit volume C_{eff}, [J/m^3K]
Graphite EPS	1.95E-06	22	15450
Slentex	1.21E-07	53	150996
Pyrogel	1.15E-07	60	178538
Geps – Pyrogel	4.90E-07	39	55285
Geps – Slentex	4.98E-07	37	52008
40 °C			
Graphite EPS	1.91E-06	25	17907
Slentex	1.23E-07	55	157639
Pyrogel	1.19E-07	63	182304
Geps – Pyrogel	5.14E-07	42	58833
Geps – Slentex	5.29E-07	40	55303

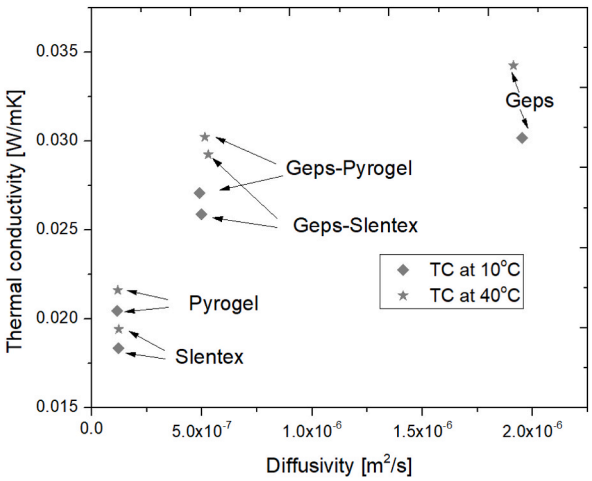

Fig. 9. Thermal conductivities in the function of the diffusivities.

a value around a constant. One can see from Fig. 10b that the highest surface temperature belongs to the graphite EPS, followed by the pyrogel, slentex and white EPS. We stopped the measurement after 120 s and the results are 75, 55, 42 and 36 °C for the graphite EPS, pyrogel, slentex and white EPS respectively. It is known that the absorption of the radiation depends on several things, such as colour, surface roughness and structure etc., which means that the sample with the darkest colour should absorb the most. But the measured temperature differences among the samples are big and significant, and it is caused not only by the dark colour. Moreover, it should be mentioned that the surface of the graphite EPS made through modification was shrunk and transformed due to the illumination, which states the good IR absorption capability of the graphite EPS presented in Fig. 1b. The investigation of the effect of irradiation on the

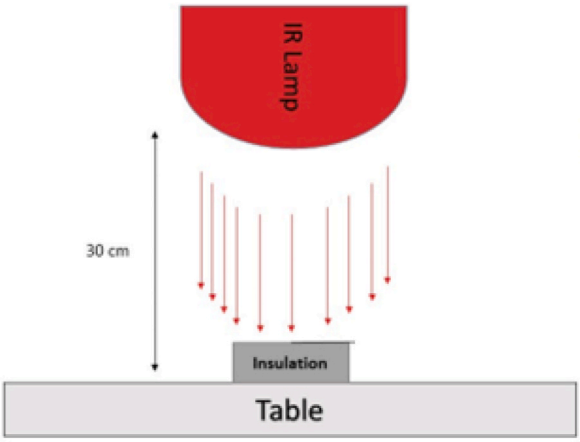

Fig. 10a. The test method for the infrared absoprtion

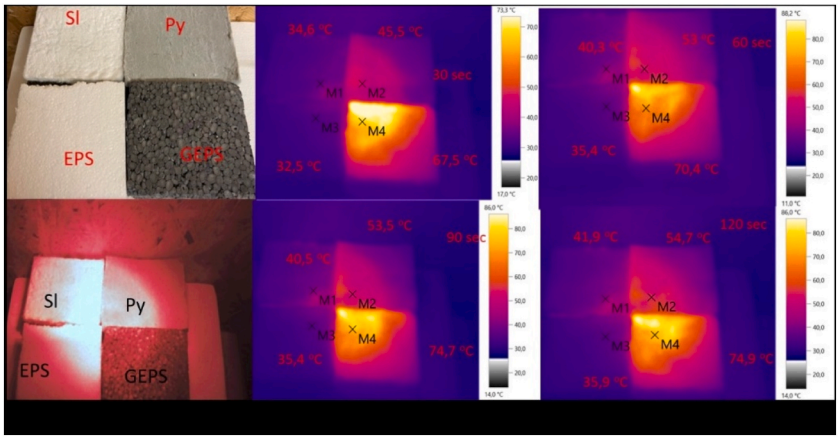

Fig. 10b. The results of infrared absorption tests.

parameters of insulation materials is momentous because strong direct sunlight may hit the sample during construction. For this, the materials such as graphite EPS should be protected from sunlight. In our country, the thermal insulation of buildings is executed in spring, autumn and surely during summer. In countries where the summer is hot and shiny the insulating of buildings should be executed rapidly, and by using shades. We must mention that examinations of aerogels with a thermo-camera prove good results from the temperature-induced changes of samples [56].

3.8. Overall comparison of the results

Finally, in Table 5 we would give an overall comparison of the measured results what can be useful for readers during their design.

Based on the measured results collected in Table 5 we could give a potential usage for the samples. It should be noticed that in an environment where humidity occurs, the use of pyrogel is not recommended, due to its high water up-taking capability. The least thermal conductivity belongs to the slentex aerogel with an advantage of about 12 and 65% compared to pyrogel and graphite EPS respectively. Based on this we recommend using slentex and pyrogel aerogels where the available space for the application is about 1–3 cm. The graphite EPS could be a good solution for application by the external wall taking into account the price. But, it should be mentioned that this material is very sensitive to both infrared waves and temperature, so during the implementation of the building, it needs special attention. The results of this paper provide a clue for researchers, designers, and decision-makers in the initial state of the construction of buildings and during the material selections. Regarding pyrogel, it is said by the manufacturer's product sheet product that it can be used for thermal insulation of the service elements of power plants. For this, as a plan, the thermal stability of the samples should be investigated in future.

4. Conclusions

These days the applications of insulation materials are more important than ever not only for buildings but for vehicles, too. The comprehensive laboratory tests of insulation materials with high performance are extremely important in both building energetics and thermal engineering. In this paper, we present a comprehensive laboratory examination completed with theoretical calculations executed on nano-structured insulation materials such as graphite EPS, slentex and pyrogel aerogel and their sandwich combinations. Moreover, as an introduction to the measurements, a very deep theoretical explanation was given also in this paper regarding the thermal conductivity of insulation materials. In this article the following interesting results were presented.

- Theoretical explanations regarding the thermal conduction in the samples were given both for the tested aerogel samples and for the graphite EPS, where the paper stated the good thermal performance of the tested materials.

Table 5
An overall collection of the results.

	GEPS	Slentex	Pyrogel
Equilibrium moisture content at 23 °C 50% [%]	0.9	0.96	1.6
Equilibrium moisture content at 23 °C 90% [%]	1.19	1.65	5.32
Contact angle [°]	100.5	110	116.5
Thermal conductivity at 10 °C [W/mK]	0.0302	0.0183	0.0205
Temperature dependency of thermal conductivity	strong	weak	weak
Specific heat capacity at 10 °C [J/kgK]	~1030	~800	~930
Infrared absorption	strong	weak	medium
Actual price	130 EUR/3m^2	235 EUR/3m^2	480 EUR/3m^2

- Moisture absorption test results showed that the pyrogel aerogel takes up the greatest amount of water among the tested three samples, while slentex and graphite EPS takes up about the same amount. Moreover, it was also manifested that this material (pyrogel) has the highest hydrophobicity value.
- The temperature dependency of the thermal conductivity as well as the temperature conversion coefficients were characterized for these samples. We stated that the thermal conductivity of the graphite EPS is the most sensitive to temperature change (fluctuation) with about 19% change in the temperature range of 0 and 40 °C. New temperature conversion coefficients were given for the tested three samples and were completed with values available in the literature.
- Results of the theoretical approximation (thickness fraction model) were compared with measurement results of the thermal conductivities of sandwich insulations (graphite EPS-pyrogel, graphite EPS-slentex). From the results we can state the use of sandwich structures is a good opportunity and the thickness ratio model for reaching the thermal conductivity of sandwich structures is perfect.
- Specific heat capacities of both the individual and sandwich samples were investigated. The results show that graphite EPS has the greatest specific heat capacity followed by the pyrogel and slentex. A mass ratio model was applied to find the specific heat capacity of the sandwich samples from the measured values of the individual samples, and the results differed from the measured values by only 2%.
- Thermal properties (diffusivity, effective heat capacity) of the samples for both individual samples and sandwich structures were calculated from the measured values. The paper states that the pyrogel insulation has the highest value of effective heat capacity, followed by the slentex and the graphite EPS both at 10 and 40 °C. It must be mentioned that the diffusivity of the sandwich structured materials approaches the diffusivity values of the individual aerogel samples.
- Infrared absorption tests proved the high infrared absorption of graphite EPS.

Authors statement

Conceptualization and supervision: Ákos Lakatos, Methodology: Ákos Lakatos, Data curation: Ákos Lakatos, Formal analysis: Ákos Lakatos, Writing—original draft preparation: Ákos Lakatos, Writing—review and editing: Ákos Lakatos, Investigation: Ákos Lakatos, Measurements: Ákos Lakatos, Funding acquisition: Ákos Lakatos, Supervision, Validation, Visualization: Ákos Lakatos.

Declaration of competing interest

The authors declare that they have no known competing financial interests or personal relationships that could have appeared to influence the work reported in this paper.

Data availability

Data will be made available on request.

Acknowledgements

This paper was supported by the János Bolyai Research Scholarship of the Hungarian Academy of Sciences, grant number: Ákos Lakatos/BO/269/20.

References

[1] U. Berardi, A cross-country comparison of the building Energy consumptions and their trends, Resour. Conserv. Recycl. 123 (2017) 230–241, https://doi.org/10.1016/j.resconrec.2016.03.014.
[2] S. Roumi, F. Zhang, R.A. Stewart, M. Santamouris, Commercial building indoor environmental quality models: a critical review, Energy Build. 263 (2022), 112033, https://doi.org/10.1016/j.enbuild.2022.112033.
[3] J. Chai, J. Fan, Advanced thermal regulating materials and systems for energy saving and thermal comfort in buildings, Mater. Today Energy 24 (2022), 100925, https://doi.org/10.1016/j.mtener.2021.100925.
[4] Y. Chen, M. Guo, Z. Chen, Z. Chen, Y. Ji, Physical energy and data-driven models in building energy prediction: a review, Energy Rep. 8 (2022) 2656–2671, https://doi.org/10.1016/j.egyr.2022.01.162.
[5] M. Khoukhi, A. Hassan, S. Al Saadi, S. Abdelbaqi, A dynamic thermal response on thermal conductivity at different temperature and moisture levels of EPS insulation, Case Stud. Therm. Eng. 14 (September 2019), 100481, https://doi.org/10.1016/j.csite.2019.100481.
[6] J. Wernery, S. Brunner, B. Weber, C. Knuth, M.M. Koebel, Superinsulation materials for energy-efficient train envelopes, Appl. Sci. 11 (7) (2021) 2939, https://doi.org/10.3390/app11072939.
[7] S. Cai, B. Zhang, L. Cremaschi, Review of moisture behavior and thermal performance of polystyrene insulation in building applications, Build. Environ. 123 (2017) 50–65, https://doi.org/10.1016/j.buildenv.2017.06.034.
[8] C. Shanshan, X. Lizhi, X. Hongyang, L. Xu, Li Zifan, C. Lorenzo, Effect of internal structure on dynamically coupled heat and moisture transfer in closed-cell thermal insulation, Int. J. Heat Mass Tran. 185 (2022), 122391, https://doi.org/10.1016/j.ijheatmasstransfer.2021.122391.
[9] S. Schiavoni, F. D'Alessandro, F. Bianchi, F. Asdrubali, Insulation materials for the building sector: a review and comparative analysis, Renew. Sustain. Energy Rev. 62 (September) (2016) 988–1011, https://doi.org/10.1016/j.rser.2016.05.045.
[10] B.P. Jelle, Traditional, state-of-the-art and future thermal building insulation materials and solutions-properties, requirements and possibilities, Energy Build. 43 (2011), https://doi.org/10.1016/j.enbuild.2011.05.015.
[11] Lakatos Á, Stability investigations of the thermal insulating performance of aerogel blanket, Energy Build. 185 (2019) 103–111, https://doi.org/10.1016/j.enbuild.2018.12.029.
[12] A. Nowoświat, P. Krause, A. Miros, Properties of expanded graphite polystyrene damaged by the impact of solar radiation, J. Build. Eng. 34 (2021), 101920, https://doi.org/10.1016/j.jobe.2020.101920.

[13] L. Török, Industry 4.0 from a few aspects, in particular, in respect of the decision making of the Management/Will the new industrial revolution change the traditional management functions, Int. Rev. Appl. Sci. Eng. 11 (2020) 140–146, https://doi.org/10.1556/1848.2020.20020.
[14] Á. Lakatos, I. Deák, U. Berardi, Thermal characterization of different graphite polystyrene, Int. Rev. Appl. Sci. Eng. 9 (2) (2018) 163–168, https://doi.org/10.1556/1848.2018.9.2.12.
[15] M.P. Tran, P. Gong, C. Detrembleur, J.M. Thomassin, P. Buahom, M. Saniei, S. Kenig, C.B. Parka, S.E. Lee, Reducing thermal conductivity of polymeric foams with high volume expansion made from polystyrene/expanded graphite, SPE ANTE (2016) 1870–1882.
[16] T. Zhang, A. Li, Q. Hari, X. Li, Y. Rao, H. Tan, S. Du, Q. Zhao, Economic thickness and life cycle cost analysis of insulating layer for the urban district steam heating pipe, Case Stud. Therm. Eng. 34 (2022), 102058, https://doi.org/10.1016/j.csite.2022.102058.
[17] A. Kan, Ni Zheng, Y. Wu, W. Wang, X. Zhang, H. Cai, D. Cao, Theoretical prediction and aging experimental verification of the service life of vacuum insulation panels, Cleaner Engineering and Technology 8 (2022), 100484, https://doi.org/10.1016/j.clet.2022.100484.
[18] Z. Fu, J. Corker, T. Papathanasiou, Y. Wang, Y. Zhou, A.O. Madyan, F. Liao, M. Fan, Critical review on the thermal conductivity modelling of silica aerogel composites, J. Build. Eng. 57 (2022), 104814, https://doi.org/10.1016/j.jobe.2022.104814.
[19] H.P. Ebert, Thermal properties of aerogels, in: A. Aegerter, N. Leventis, M. Koebel (Eds.), Aerogels Handbook, Springer, New York, NY, USA, 2011, pp. 537–564, https://doi.org/10.1007/978-1-4419-7589-8_23.
[20] K. Ghazi Wakili, Th Stahl, E. Heiduk, M. Schuss, R. Vonbank, U. Pont, C. Sustr, D. Wolosiuk, D. Mahdavi, High performance aerogel containing plaster for historic buildings with structured façades, En. Proc. 78 (2015) 949–954, https://doi.org/10.1016/j.egypro.2015.11.027.
[21] H. Liu, J. Liu, Y. Tian, X. Wu, Z. Li, Investigation of high temperature thermal insulation performance of fiber-reinforced silica aerogel composites, Int. J. Therm. Sci. 183 (2022), 107827, https://doi.org/10.1016/j.ijthermalsci.2022.107827.
[22] K.R. Pyun, S.H. Ko, Graphene as a material for energy generation and control: recent progress in the control of graphene thermal conductivity by graphene defect engineering, Mater. Today Energy 12 (2019) 431–442, https://doi.org/10.1016/j.mtener.2019.04.008.
[23] Krause, P., Nowoświat, A. Experimental studies involving the impact of solar radiation on the properties of expanded graphite polystyrene Energies 13(1),75 https://doi.org/10.3390/en13010075.
[24] Á. Lakatos, A. Csík, Multiscale thermal investigations of graphite doped polystyrene thermal insulation, Polymers 14 (8) (2022), https://doi.org/10.3390/polym14081606 art. no. 1606.
[25] H.M. Danaci, N. Akin, Thermal insulation materials in architecture: a comparative test study with aerogel and rock wool, Environ. Sci. Pollut. Res. 29 (2022) 72979–72990, https://doi.org/10.1007/s11356-022-20927-2.
[26] A. Karanafti, T. Theodosiou, K. Tsikalouda, Assessment of buildings' dynamic thermal insulation technologies-A review, Appl. Energy 326 (2022), 119985, https://doi.org/10.1016/j.apenergy.2022.119985.
[27] R. Landolfi, M. Nicolella, Durability assessment of ETICS: comparative evaluation of different insulating materials, Sustainability 14 (2) (2022) 980, https://doi.org/10.3390/su14020980.
[28] L.M. Moga, A. Bucur, I. Iancu, Current Practices in Energy Retrofit of Buildings, Springer Tracts Civ Eng, 2021, pp. 1–41, https://doi.org/10.1007/978-3-030-57418-5_1.
[29] S. Cai, W. Zhu, L. Cremaschi, Study of the meso-structure and its impact on the thermal performance of closed-cell insulation with moisture ingress, Procedia Eng. 205 (2017) 2823–2830, https://doi.org/10.1016/j.proeng.2017.09.899.
[30] A. Bucur, L.M. Moga, D.L. Manea, Investigations on the hygrothermal properties of aerogel insulation blankets, lecture notes in networks and systems 386 LNNS, in: 15th International Conference on Interdisciplinarity in Engineering, INTER-ENG, 2021, pp. 455–4652022, https://doi.org/10.1007/978-3-030-93817-8_42.
[31] Á. Lakatos, A. Csík, I. Csarnovics, Experimental verification of thermal properties of the aerogel blanket, Case Stud. Therm. Eng. 25 (2021), 100966, https://doi.org/10.1016/j.csite.2021.100966.
[32] Y. Liao, X. Wu, H. Liu, Y. Chen, Thermal conductivity of powder silica hollow spheres, Thermochim. Acta 526 (1–2) (2011) 178–184, https://doi.org/10.1016/j.tca.2011.09.011.
[33] B.P. Jelle, B.G. Tilset, T. Gao, M. Grandcloas, O.M. Lovvik, R.A. Bohne, A.S. Mofid, S. Ng, E. Sagvolden, High-performance nano insulation materials for energy-efficient buildings, in: Conference: Proceedings of TechConnect World Innovation Conference 2017, 2017, pp. 289–292. Washington DC, USA, 14-17 May, 2017. At: Washington DC, USA.
[34] B. Mosavati, M. Mosavati, F. Kowsary, Solution of radiative inverse boundary design problem in a combined radiating-free convecting furnace, Int. Commun. Heat Mass Tran. 45 (2013) 130–136, https://doi.org/10.1016/j.icheatmasstransfer.2013.04.011.
[35] A. Nowoświat, P. Krause, A. Miros, Properties of expanded graphite polystyrene damaged by the impact of solar radiation, J. Build. Eng. 34 (2021), 101920, https://doi.org/10.1016/j.jobe.2020.101920.
[36] F. He, Y. Wang, W. Zheng, J.Y. Wu, Y.H. Huang, Effective thermal conductivity model of aerogel thermal insulation composite, Int. J. Therm. Sci. 179 (2022), 107654, https://doi.org/10.1016/j.ijthermalsci.2022.107654.
[37] X. Style Wang, P. Xie, K. Wan, Y. Miao, Z. Liu, X. Li, C. Wang, Mechanically strong, low thermal conductivity and improved thermal stability polyvinyl alcohol-graphene-nanocellulose aerogel, Gels 7 (4) (2021) 170, https://doi.org/10.3390/gels7040170.
[38] G. Gróf, Notes on using temperature-dependent thermal diffusivity-forgotten rules, J. Therm. Anal. Calorim. 132 (2) (2018) 1389–1397, https://doi.org/10.1007/s10973-018-7014-4, 8 pp.
[39] A. Salazar, On thermal diffusivity, Eur. J. Phys. 24 (4) (2003) 351, https://doi.org/10.1088/0143-0807/24/4/353.
[40] H.S. Park, B.K. Oh, T. Cho, Compressive properties of graphite-embedded expanded polystyrene for vibroacoustic engineering applications, Compos. B Eng. 93 (2016) 252–264, https://doi.org/10.1016/j.compositesb.2016.03.004.
[41] M. Xiao, L. Sun, J. Liu, Y. Li, K. Gong, Synthesis and properties of polystyrene/graphite nanocomposites, Polymer 43 (2002) 2245–2248, https://doi.org/10.1016/S0032-3861(02)00022-8.
[42] C. Zhang, X. Li, S. Chen, R. Yang, Effects of graphite on styrene suspension polymerization and flame retarded expandable polystyrene, Gongcheng/Polym. Mater. Sci. Eng. 32 (2016) 6–11.
[43] A. Blazejczyk, C. Jastrzebski, M. Wierzbicki, Change in conductive-radiative heat transfer - mechanism forced by graphite microfiller, in expanded polystyrene thermal, insulation-experimental and simulated investigations, Materials 13 (2020) 2626, https://doi.org/10.3390/ma13112626.
[44] http://www.aerogelszigeteles.hu/system/files/Spaceloft_DS_1.1.pdf.
[45] ISO 12571, Hygrothermal Performance of Building Materials and Products - Determination of Hygroscopic Sorption Properties, 2013.
[46] J. Pan, F. Chen, D.E. Cabrera, Z. Min, S. Ruan, M. Wu, D. Zhang, J.M. Castro, J.L. Lee, Carbon particulate and controlled-hydrolysis assisted extrusion foaming of semicrystalline polyethylene terephthalate for the enhanced thermal insulation property, J. Cell. Plast. 57 (2021) 695–716, https://doi.org/10.1177/0021955X20952751.
[47] J. Pan, D. Zhang, M. Wu, S. Ruan, J.M. Castro, J.L. Lee, F. Chen, Impacts of carbonaceous particulates on extrudate semicrystalline polyethylene terephthalate foams: nonisothermal crystallization, rheology, and infrared attenuation studies, Ind. Eng. Chem. Res. 59 (2020) 15586–15597, https://doi.org/10.1021/acs.iecr.0c02929.
[48] S. Brunauer, L.S. Deming, E. Teller, On a theory of Van der Waals adsorption of gases, J. Am. Chem. Soc. 62 (7) (1940) 1723–1732, https://doi.org/10.1021/ja01864a025.
[49] Xuejie Yue, Hai Wu, Tao Zhang, Dongya Yang, Fengxian Qiu, Superhydrophobic waste paper-based aerogel as a thermal insulating cooler for building, Energy 245 (2022), 123287, https://doi.org/10.1016/j.energy.2022.123287.
[50] V. Novak, J. Zach, Study of the efficiency and durability of hydrophobization modifications of building elements, IOP Conf. Ser. Mater. Sci. Eng. 583 (2019), 012032, https://doi.org/10.1088/1757-899X/583/1/012032.
[51] Berardi U., Naldi M., The impact of the temperature dependent thermal conductivity of insulating materials on the effective building envelope performance, Energy Build., 144: 262-275. https://doi.org/10.1016/j.enbuild.2017.03.052.

[52] EN ISO 10456: 277 standard: Building materials and products. Hygrothermal Properties. Tabulated Design Values and Procedures for Determining Declared and Design Thermal Values.
[53] Y. Ding, S.X. Zhou, S.E. Huang, Z.P. Wang, Y.Q. Wei, Determination of thermal conductivity coefficient of composite materials based on 3D simulation of COMSOL, Transducer. Microsystem Tech. 37 (9) (2018) 112–113, 116. (in Chinese).
[54] Á. Lakatos, Basics of Heat Transfer and Fluid Mechanics, University of Debrecen, 2014, ISBN 9789634737988, p. 126.
[55] X. Zhang, Y. Wang, Y. Wang, B. Liu, X. Bai, Preliminary study on the thermal insulation of a multilayer passive thermal protection system with carbon-phenolic composites in a combustion chamber, Case Stud. Therm. Eng. 35 (2022), 102120, https://doi.org/10.1016/j.csite.2022.102120.
[56] X. Zhang, Y. Jiang, X. Xu, H. Liu, N. Wu, C. Han, B. Wang, Y. Wang, Thermal stable, fire-resistant and high strength SiBNO fiber/SiO2 aerogel composites with excellent thermal insulation and wave-transparent performances, Mater. Today Commun. 33 (2022), 104261, https://doi.org/10.1016/j.mtcomm.2022.104261.